Experimental Determination of Phase Equilibria in the Co-Cr-V Ternary System

C.C. Zhao, Y. Yu, X.J. Liu, and C.P. Wang

The phase equilibria in the Co-Cr-V ternary system were investigated by means of optical microscopy, electron probe microanalysis and x-ray diffraction. Four isothermal sections of the Co-Cr-V ternary system at 800, 1000, 1100 and 1200 °C were established. The experimental results show that: (1) no ternary compound was found in this system; (2) the σ and (V, Cr) phases form the continuous solid solutions from the Co-Cr side to Co-V side in the isothermal sections at 800-1200 °C.

1. Introduction

The Co-Cr base alloys have been widely used as commercial magnetic recording materials,[1-4] and the Co-V system is a potential candidate of ultra-high density recording media because of phase separation between the ferromagnetic hcp phase and non-magnetic hcp phase,[5] which is similar to the Co-Cr system. Thus, the Co-Cr-V ternary alloys as promising magnetic recording materials, are of both technical importance and academic interest. The properties of alloy materials are affected by the microstructure and composition. In order to properly understand the relationship between magnetic properties and microstructure, accurate information on the phase equilibria in the Co-Cr-V ternary system is required. However, only an isothermal section at 1150 °C in the Co-Cr-V system reported by Kuznetsov et al.[6] was available. Therefore, it is important to comprehensively determine the phase equilibria in the Co-Cr-V ternary system.

The Co-Cr binary system has been studied by many researchers,[7-9] the latest version experimentally investigated and thermodynamically calculated by Oikawa et al.[9] shows five phases ((αCo), (εCo), (Cr), L, and σ-Cr₃Co₂), and a magnetically induced phase separation of the ferromagnetic (α_fCo) and the paramagnetic (α_pCo) in the range of 764-965 °C. The melting point of the σ-Cr₃Co₂ phase is about 1280 °C.[9] Some researchers investigated the phase
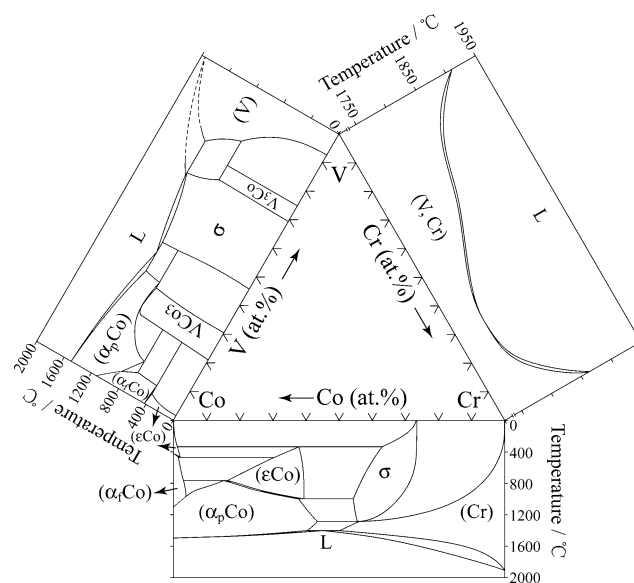
C.C. Zhao, Y. Yu, X.J. Liu, and **C.P. Wang**, Department of Materials Science and Engineering, College of Materials, and Research Center of Materials Design and Applications, Xiamen University, Xiamen 361005, People's Republic of China. Contact e-mail: wangcp@xmu. edu.cn.
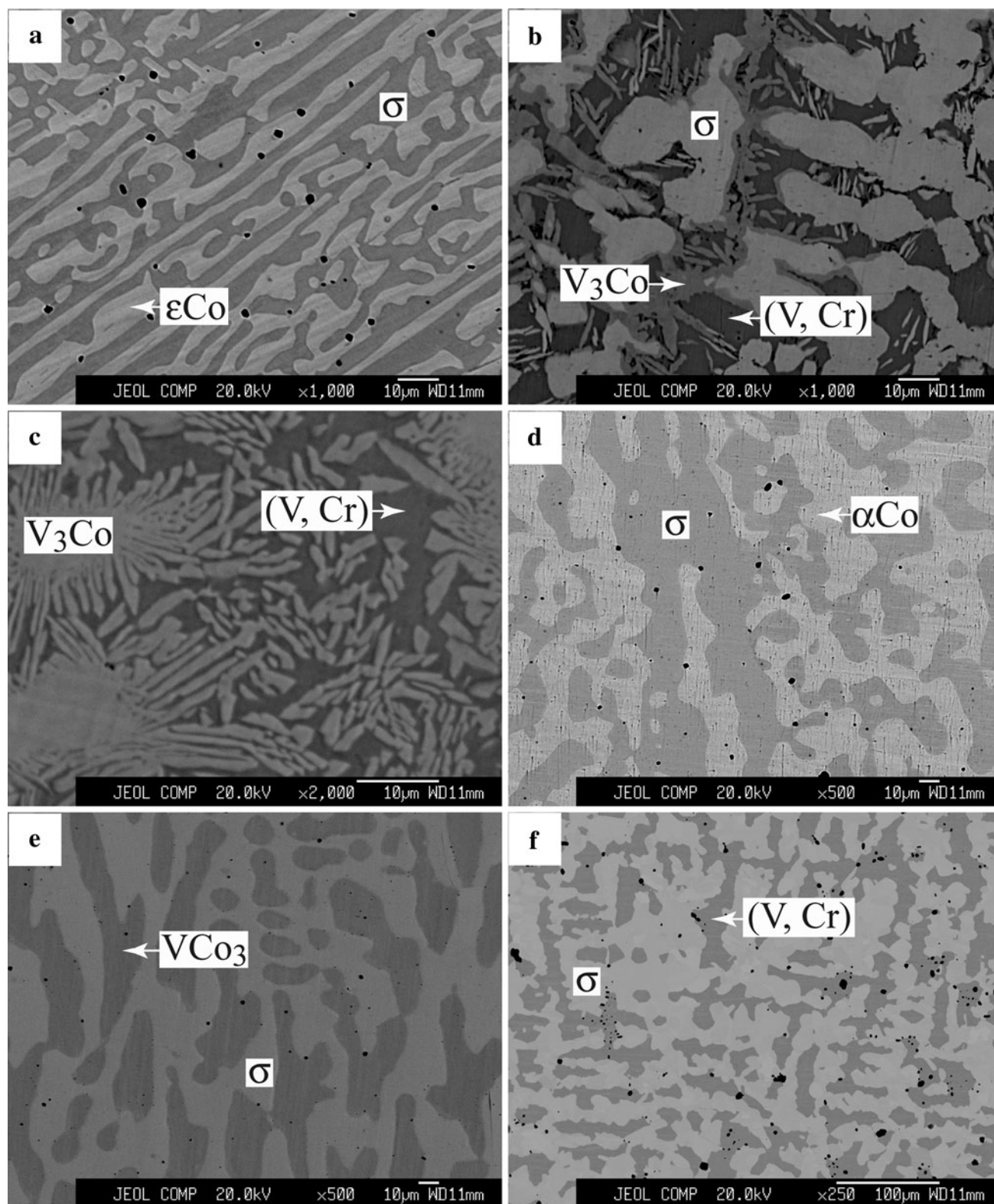
Fig. 1 Binary phase diagrams constituting the Co-Cr-V ternary system[5,9,13]

Table 1 Stable solid phases in the three binary systems

System	Phase	Pearson's symbol	Prototype	Strukturbericht	Reference
Co-Cr	(αCo)	cF4	Cu	A1	[9]
	(εCo)	hP2	Mg	A3	[9]
	(Cr)	cI2	W	A2	[9]
	σ	tP30	σCrFe	D8_b	[9]
Co-V	(αCo)	cF4	Cu	A1	[5]
	(εCo)	hP2	Mg	A3	[5]
	VCo₃	hP24	VCo₃	…	[5]
	σ	tP30	σCrFe	D8_b	[5]
	V₃Co	cP8	SiCr₃	A15	[5]
	(V)	cI2	W	A2	[5]
Cr-V	(V, Cr)	cI2	W	A2	[13]

Fig. 2 BSE images of typical Co-Cr-V ternary alloys: (a) Co56:Cr40:V4 (at.%) alloy annealed at 800 °C for 90 days; (b) Co24:Cr12:V64 (at.%) alloy annealed at 800 °C for 90 days; (c) Co20:Cr4:V76 (at.%) alloy annealed at 800 °C for 90 days; (d) Co56:Cr40:V4 (at.%) alloy annealed at 1000 °C for 60 days; (e) Co64:Cr5:V31 (at.%) alloy annealed at 1000 °C for 60 days and (f) Co29:Cr67:V4 (at.%) alloy annealed at 1100 °C for 45 days
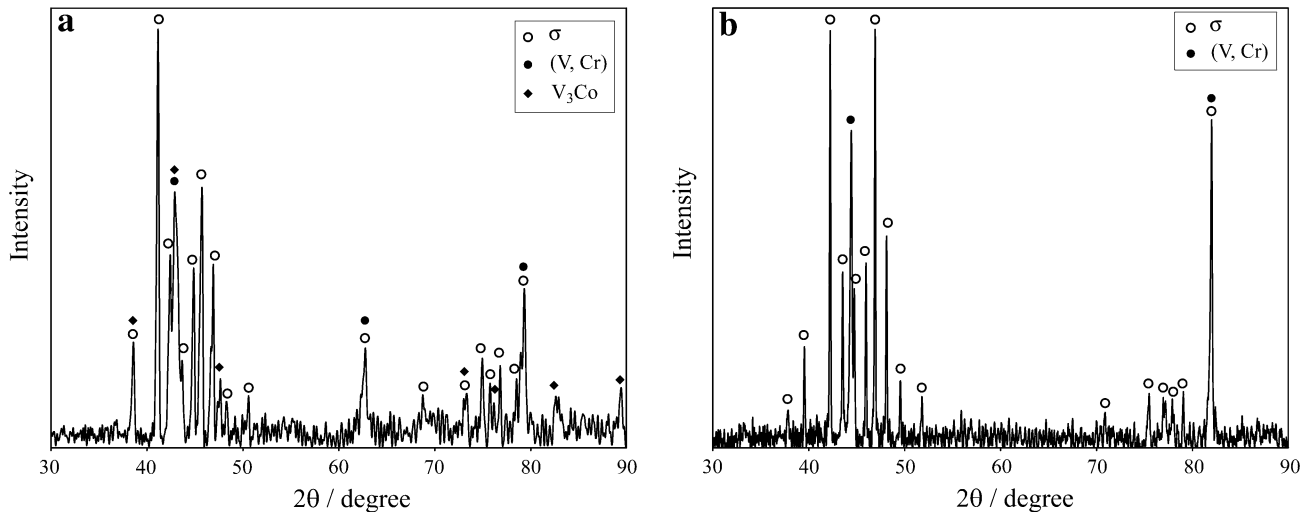
Fig. 3 XRD patterns obtained from (a) Co24:Cr12:V64 (at.%) alloy annealed at 800 °C for 90 days and (b) Co29:Cr67:V4 (at.%) alloy annealed at 1100 °C for 45 days

diagram of the Co-V system,[5,10-12] but the Co-V diagram assessed by Okamoto[5] in 2006 was more consistent with the experimental data of the present work. In the Co-V binary system, there are three intermetallic phases (VCo$_3$, σ-V$_3$Co$_2$, and V$_3$Co) and a magnetically induced (αCo) phase separation of the ferromagnetic (α$_f$Co) and the paramagnetic (α$_p$Co) from 691 to 873 °C. The transformation temperature from the (αCo) to VCo$_3$ is reported to be 1045 °C.[5] The Cr-V binary system is a simple system without any intermediate phase.[13] The three sub-binary systems, Co-Cr, Co-V and Cr-V, are shown in Fig. 1. The stable solid phases in the three binary systems are summarized in Table 1.

The objective of the present work is to experimentally investigate the phase equilibria in the Co-Cr-V ternary system using optical microscopy (OM), electron probe microanalysis (EPMA) and x-ray diffraction (XRD). The experimental results are expected to help in understanding the microstructures of promising Co-Cr-V alloys and provide key support for the thermodynamic assessment of this system and the design of related material.

2. Experimental Procedure

Cobalt (99.9 wt.%), chromium (99.7 wt.%) and vanadium (99.7 wt.%) were used as starting materials. Bulk buttons were prepared from pure elements by arc melting under high purity argon atmosphere using a non-consumable tungsten electrode. The ingots were melted 6 times in order to achieve homogeneity. The sample weight was around 20 g and the weight loss during melting was generally less than 0.20%. Afterwards, the ingots were cut into small pieces for heat treatment and further observations. Plate-shaped specimens were put into quartz

ampoules evacuated and backfilled with argon gas, then annealed in the temperature range from 800 to 1200 °C. The samples were annealed at 800, 1000, 1100 and 1200 °C for 90, 60, 45 and 20 days, respectively. At the end of the heat treatment, the specimens were quenched into iced water.

After standard metallographic preparation, microstructural observation of specimens was carried out by OM. The compositions (assumed to be equilibrium) of each phase in the annealed alloys were determined by EPMA (JXA-8100R, JEOL, Japan). Pure elements were used as standards, and the measurements were carried out at 20 kV. Every phase was analyzed seven times in different regions, and its composition was averaged. The XRD was used to identify the crystal structure of the constituent phase. The XRD measurements were carried out on a Phillips Panalytical X-pert diffractometer using Cu-K$_\alpha$ radiation at 40 kV and 30 mA. The data were collected in the range of 2θ from 20° to 90° at a step width of 0.0167°.

3. Results and Discussion

3.1 Microstructural Morphologies

Back-scattered electron (BSE) images of the typical ternary Co-Cr-V alloys are presented in Fig. 2. Phase identification was based on the composition as measured by EPMA and the XRD results. The two-phase equilibrium σ + (εCo) was identified in the Co56:Cr40:V4 (at.%) alloy annealed at 800 °C for 90 days, and is shown in Fig. 2(a), where the σ phase is dark gray and the (εCo) phase is light gray. In the Co24:Cr12:V64 (at.%) alloy annealed at 800 °C for 90 days, the three-phase microstructure VCo$_3$ + σ + (V, Cr) was observed (Fig. 2b) and substantiated by the XRD results in Fig. 3(a). The finer needles in the dark (V, Cr)

Table 2 Analyzed compositions of the annealed alloys

Temp., °C	Alloys, at.%	Overall composition, at.%	Phase equilibria Phase 1/phase 2/phase 3	Phase 1 Cr	Phase 1 V	Phase 2 Cr	Phase 2 V	Phase 3 Cr	Phase 3 V
800	Co92:Cr4:V4	Co91.7:Cr4.1:V4.2	αCo	4.1 ± 0.02	4.2 ± 0.15				
	Co79:Cr4:V17	Co78.8:Cr4.2:V17.0	αCo/VCo₃	5.0 ± 0.16	12.9 ± 0.40	4.6 ± 0.15	17.4 ± 0.45		
	Co76:Cr16:V8	Co75.6:Cr16.3:V8.1	εCo	16.3 ± 0.07	8.1 ± 0.10				
	Co70:Cr20:V10	Co70.6:Cr19.9:V9.5	εCo	19.9 ± 0.15	9.5 ± 0.09				
	Co70:Cr17:V13	Co69.5:Cr17.2:V13.3	εCo/VCo₃	18.6 ± 0.27	12.4 ± 0.34	14.8 ± 0.53	15.2 ± 0.07		
	Co60:Cr4:V36	Co60.1:Cr4.2:V35.7	VCo₃/σ	1.7 ± 0.12	27.7 ± 0.14	5.9 ± 0.12	39.9 ± 0.32		
	Co60:Cr12:V28	Co59.8:Cr12.0:V28.2	VCo₃/σ	6.7 ± 0.23	25.2 ± 0.56	18.3 ± 0.08	30.6 ± 0.24		
	Co60:Cr20:V20	Co59.4:Cr20.6:V20.0	VCo₃/σ	8.8 ± 0.13	21.4 ± 0.08	29.7 ± 0.85	19.2 ± 0.05		
	Co60:Cr32:V8	Co59.6:Cr32.1:V8.3	εCo/σ	26.6 ± 0.60	7.4 ± 0.37	42.1 ± 0.23	9.5 ± 0.05		
	Co56:Cr40:V4	Co55.8:Cr40.1:V4.1	εCo/σ	31.4 ± 0.04	3.4 ± 0.02	48.9 ± 0.47	4.3 ± 0.22		
	Co27:Cr8:V65	Co27.4:Cr8.2:V64.4	σ/V₃Co	7.5 ± 0.19	62.0 ± 0.21	10.4 ± 0.43	65.3 ± 0.70		
	Co24:Cr12:V64	Co23.8:Cr12.3:V63.9	σ/V₃Co/(V, Cr)	9.9 ± 0.12	60.0 ± 0.17	11.8 ± 0.56	64.1 ± 0.07	15.4 ± 0.15	65.9 ± 0.30
	Co26:Cr32:V42	Co26.6:Cr31.3:V42.1	σ/(V, Cr)	26.6 ± 0.15	41.9 ± 0.24	39.3 ± 0.13	42.9 ± 0.34		
	Co20:Cr60:V20	Co21.4:Cr58.1:V20.5	σ/(V, Cr)	44.1 ± 0.82	22.6 ± 0.57	66.7 ± 0.06	19.5 ± 0.03		
	Co20:Cr20:V60	Co19.8:Cr19.8:V60.4	σ/(V, Cr)	13.2 ± 0.27	56.5 ± 0.28	23.3 ± 0.14	60.7 ± 0.11		
	Co20:Cr76:V4	Co20.8:Cr75.1:V4.2	σ/(V, Cr)	61.0 ± 0.06	4.6 ± 0.20	80.4 ± 0.16	3.7 ± 0.25		
	Co20:Cr4:V76	Co19.8:Cr4.4:V75.8	V₃Co/(V, Cr)	4.1 ± 0.26	72.1 ± 0.20	7.1 ± 0.15	82.5 ± 0.40		
	Co19:Cr11:V70	Co19.0:Cr11.4:V69.6	V₃Co/(V, Cr)	10.2 ± 0.83	67.1 ± 0.34	12.6 ± 0.17	70.0 ± 0.22		
1000	Co79:Cr4:V17	Co78.6:Cr4.2:V17.2	αCo	4.2 ± 0.09	17.2 ± 0.08				
	Co70:Cr6:V24	Co69.4:Cr6.3:V24.3	αCo	6.3 ± 0.09	24.3 ± 0.05				
	Co70:Cr20:V10	Co70.5:Cr20.0:V9.5	αCo	20.0 ± 0.09	9.5 ± 0.08				
	Co64:Cr5:V31	Co64.6:Cr4.9:V30.5	αCo/σ	4.2 ± 0.06	28.2 ± 0.17	6.7 ± 0.13	34.1 ± 0.09		
	Co60:Cr12:V28	Co60.0:Cr11.9:V28.1	αCo/σ	8.8 ± 0.26	24.2 ± 0.35	13.6 ± 0.28	29.0 ± 0.32		
	Co60:Cr20:V20	Co60.2:Cr19.9:V19.9	αCo/σ	15.6 ± 0.08	17.7 ± 0.19	23.6 ± 0.05	21.8 ± 0.09		
	Co56:Cr40:V4	Co55.7:Cr40.4:V3.9	αCo/σ	33.3 ± 0.20	3.6 ± 0.05	47.4 ± 0.34	4.3 ± 0.12		
	Co26:Cr32:V42	Co26.3:Cr31.5:V42.2	σ/(V, Cr)	26.3 ± 0.13	42.4 ± 0.08	45.2 ± 0.48	40.9 ± 0.54		
	Co20:Cr4:V76	Co19.6:Cr4.9:V75.5	σ/(V, Cr)	3.8 ± 0.09	68.1 ± 0.13	6.5 ± 0.25	77.7 ± 0.17		
	Co20:Cr20:V60	Co20.2:Cr20.0:V59.8	σ/(V, Cr)	13.5 ± 0.24	56.2 ± 0.19	23.9 ± 0.17	60.2 ± 0.25		
	Co20:Cr60:V20	Co21.0:Cr58.8:V20.2	σ/(V, Cr)	44.7 ± 0.08	21.8 ± 0.13	68.1 ± 0.14	18.9 ± 0.16		
	Co20:Cr76:V4	Co21.0:Cr74.6:V4.4	σ/(V, Cr)	61.3 ± 0.15	4.8 ± 0.06	81.0 ± 0.07	3.6 ± 0.08		
1100	Co64:Cr5:V31	Co64.2:Cr5.2:V30.6	αCo/σ	4.7 ± 0.19	28.5 ± 0.18	6.6 ± 0.16	34.6 ± 0.19		
	Co60:Cr20:V20	Co59.5:Cr21.4:V19.1	αCo/σ	18.6 ± 0.08	16.3 ± 0.30	25.5 ± 0.17	20.4 ± 0.33		
	Co56:Cr40:V4	Co5.1:Cr40.9:V4.0	αCo/σ	35.1 ± 0.12	3.5 ± 0.12	47.6 ± 0.66	4.3 ± 0.09		
	Co29:Cr67:V4	Co28.3:Cr67.6:V4.1	σ/(V, Cr)	62.3 ± 0.19	4.0 ± 0.14	75.5 ± 0.13	3.3 ± 0.05		
	Co28:Cr53:V19	Co28.5:Cr52.9:V18.6	σ/(V, Cr)	48.4 ± 0.13	18.6 ± 0.07	65.6 ± 0.21	16.8 ± 0.13		
	Co26:Cr32:V42	Co25.9:Cr32.1:V42.0	σ/(V, Cr)	26.5 ± 0.48	42.0 ± 0.40	40.9 ± 0.50	41.6 ± 0.48		
	Co25:Cr20:V55	Co25.2:Cr20.0:V54.8	σ/(V, Cr)	16.4 ± 0.10	53.0 ± 0.16	25.2 ± 0.05	56.3 ± 0.09		
	Co24:Cr12:V64	Co23.9:Cr12.3:V63.7	σ/(V, Cr)	9.9 ± 0.03	59.9 ± 0.10	15.3 ± 0.17	66.1 ± 0.45		
1200	Co60:Cr4:V36	Co60.0:Cr4.3:V35.7	αCo/σ	3.5 ± 0.03	29.9 ± 0.07	4.8 ± 0.05	36.0 ± 0.16		
	Co60:Cr20:V20	Co59.7:Cr20.0:V20.3	αCo/σ	17.7 ± 0.09	18.4 ± 0.14	23.6 ± 0.19	22.1 ± 0.17		
	Co56:Cr40:V4	Co55.3:Cr40.6:V4.0	αCo/σ	36.6 ± 0.19	3.5 ± 0.03	47.9 ± 0.14	4.2 ± 0.14		
	Co29:Cr67:V4	Co28.8:Cr67.2:V4.0	σ/(V, Cr)	61.3 ± 0.13	4.1 ± 0.06	70.2 ± 0.28	3.5 ± 0.09		
	Co28:Cr53:V19	Co27.3:Cr53.6:V19.1	σ/(V, Cr)	47.2 ± 0.18	19.5 ± 0.26	58.1 ± 0.27	18.5 ± 0.15		
	Co26:Cr32:V42	Co25.9:Cr32.1:V42.0	σ/(V, Cr)	26.3 ± 0.14	41.8 ± 0.07	35.8 ± 0.56	41.8 ± 0.41		
	Co25:Cr20:V55	Co24.5:Cr21.5:V53.9	σ/(V, Cr)	18.4 ± 0.04	49.9 ± 0.03	24.6 ± 0.08	54.3 ± 0.16		
	Co24:Cr12:V64	Co23.9:Cr1.12:V63.9	σ/(V, Cr)	9.5 ± 0.13	59.5 ± 0.11	13.2 ± 0.08	64.1 ± 0.07		

phase were confirmed to be the σ phase by EPMA and XRD analysis. The two-phase microstructure V₃Co + (V, Cr) of the Co20:Cr4:V76 (at.%) alloy annealed at 800 °C for 90 days is shown in Fig. 2(c), with V₃Co being the dendrites. In addition, the varying contrast in the dark gray (V, Cr) phase may be caused by the coring in the alloy samples, or the different crystal orientation of the bcc (V, Cr) phase. Figure 2(d) shows the two-phase microstructure

σ + (αCo) in the Co56:Cr40:V4 (at.%) alloy annealed at 1000 °C for 60 days. Figure 2(e) shows the two-phase microstructure σ + V₃Co of the Co64:Cr5:V31 (at.%) alloy annealed at 1000 °C for 60 days, where the dendrites were VCo₃. In the Co29:Cr67:V4 (at.%) alloy annealed at 1100 °C for 45 days, σ and (V, Cr) were identified, as shown in Fig. 2(f), and XRD presented in Fig. 3(b) confirmed these phases.

3.2 Isothermal Sections

The analyzed compositions of the Co-Cr-V ternary system at 800, 1000, 1100 and 1200 °C determined by EPMA are listed in Table 2. Using these experimental data, the isothermal sections at 800, 1000, 1100 and 1200 °C were constructed in Fig. 4-7. In all cases, the overall

composition was on the tie line in the two phase samples. At 800 °C, Fig. 4, there are four single-phase regions: (αCo), (εCo), VCo₃, (V, Cr), and σ, and one determined three-phase region σ + (V, Cr) + V₃Co. Two three-phase equilibria: (αCo) + (εCo) + VCo₃, (εCo) + VCo₃ + σ and the phase separation of (α_fCo) + (α_pCo), shown as dashed lines were inferred, and were not found in the current samples. The σ and (V, Cr) phases formed continuous solid solutions from the Co-Cr side to Co-V side, and V₃Co behaved as a line compound.

The isothermal section at 1000 °C is shown in Fig. 5, where four two-phase regions (αCo) + VCo₃, (αCo) + σ,
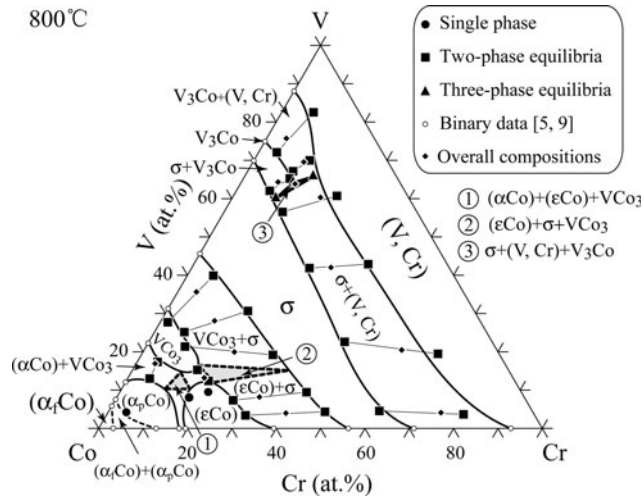

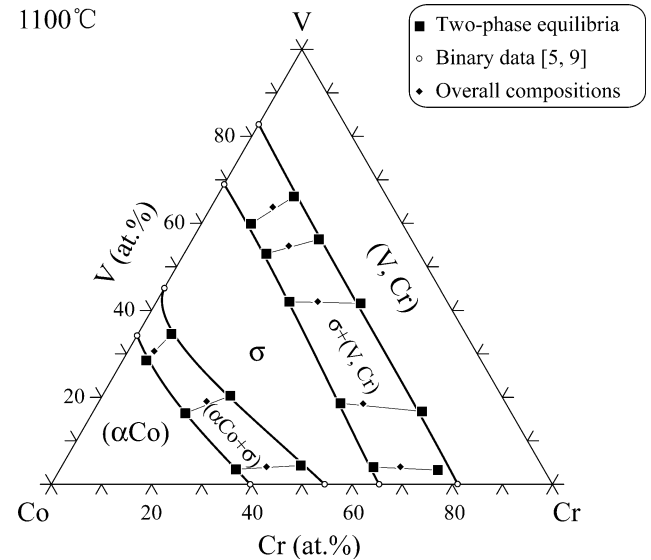**Fig. 4** Experimentally determined isothermal section of the Co-Cr-V system at 800 °C

Fig. 6 Experimentally determined isothermal section of the Co-Cr-V system at 1100 °C
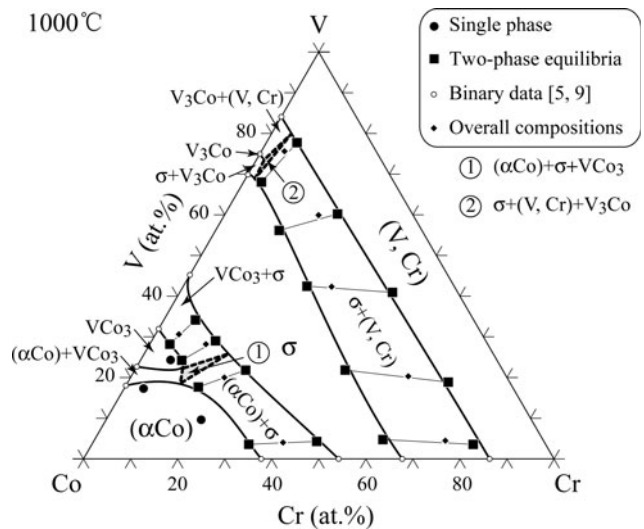

Fig. 5 Experimentally determined isothermal section of the Co-Cr-V system at 1000 °C
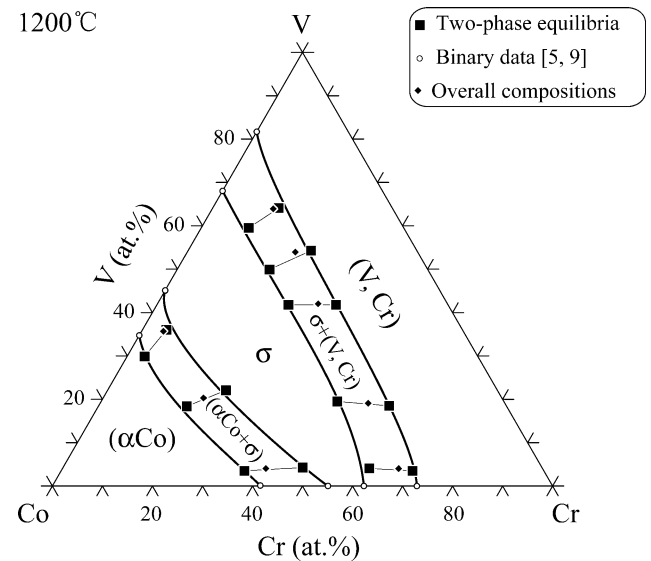

Fig. 7 Experimentally determined isothermal section of the Co-Cr-V system at 1200 °C

$VCo_3 + \sigma$, and $\sigma + (V, Cr)$ were identified. The VCo_3 and V_3Co phases at 1000 °C (Fig. 5), disappeared at 1100 °C (Fig. 6), where only three single-phase regions (αCo), (V, Cr), and σ and two two-phase regions (αCo) + σ, and $\sigma + (V, Cr)$ appeared. The phase relationship shown in the isothermal section at 1200 °C (Fig. 7) is similar to that at 1100 °C, although the solubilities of phases were slightly different, due to the different temperatures. It should be noted that not all phase boundaries were drawn through the data points in Fig. 4-7, especially for Fig. 4. This is likely to be because the phases had not attached equilibrium, or that the boundaries were actually more curved than indicated on the figures.

4. Conclusions

Four isothermal sections of the Co-Cr-V ternary system at 800, 1000, 1100 and 1200 °C were experimentally determined. No ternary compound was found in this system. The σ and (V, Cr) phases formed continuous solid solutions from the Co-Cr side to Co-V side at all temperatures examined.

References

1. M.L. Plumer, J. Van Ek, and D. Weller, *The Physics of Ultra-High-Density Magnetic Recording*, Springer, New York, 2001
2. S. Khizroev and D. Litvinov, *Perpendicular Magnetic Recording*, Kluwer Academic, Boston, 2004
3. C.D. Mee and E.D. Daniel, *Magnetic Recording Technology*, McGraw-Hill, New York, 1996
4. E.D. Daniel, C.D. Mee, and M.H. Clark, *Magnetic Recording: The First 100 Years*, IEEE Press, New York, 1999
5. H. Okamoto, Co-V (Cobalt-Vanadium), *J. Phase Equilib. Diffus.*, 2006, **27**(2), p 198
6. V.N. Kuznetsov, G.P. Zhmurko, Zh.N. Toibayev, K.B. Kalmykov, L.M. Aziyeva, and L.S. Guzei, Experimental Research and Thermodynamic Simulation of Phase Equilibria in Co-Cr-V System, *Mosc. Univ. Chem. Bull.*, 2001, **42**, p 121-124, in Russian
7. A. Kusoffsky and B. Jansson, A Thermodynamic Evaluation of the Co-Cr and the C-Co-Cr Systems, *CALPHAD*, 1997, **21**(3), p 321-333
8. K. Ishida and T. Nishizawa, The Co-Cr (Cobalt-Chromium) System, *J. Phase Equilib.*, 1990, **11**(4), p 357-370
9. K. Oikawa, G.W. Qin, T. Ikeshoji, R. Kainuma, and K. Ishida, Direct Evidence of Magnetically Induced Phase Separation in the FCC Phase and Thermodynamic Calculations of Phase Equilibria of the Co-Cr System, *Acta Mater.*, 2002, **50**(9), p 2223-2232
10. H. Okamoto, Co-V (Cobalt-Vanadium), *J. Phase Equilib. Diffus.*, 2007, **28**(3), p 314
11. S.G. Huang, L. Li, O. Van der Biest, and J. Vleugels, Thermodynamic Assessment of the Co-V and Co-V-C System, *J. Alloys Compd.*, 2004, **385**(1-2), p 114-118
12. J. Smith, The Co-V (Cobalt-Vanadium) System, *J. Phase Equilib.*, 1991, **12**(3), p 324-331
13. J.F. Smith, *Phase Diagrams of Binary Vanadium Alloys*, ASM International, Materials Park, OH, 1989